



## Crosstalk in 1.5- $\mu$ m InGaAsP optical amplifiers

Lassen, H. E.; Hansen, Peter Bukhave; Stubkjær, Kristian

*Published in:*  
Journal of Lightwave Technology

*Link to article, DOI:*  
[10.1109/50.7916](https://doi.org/10.1109/50.7916)

*Publication date:*  
1988

*Document Version*  
Publisher's PDF, also known as Version of record

[Link back to DTU Orbit](#)

*Citation (APA):*  
Lassen, H. E., Hansen, P. B., & Stubkjær, K. (1988). Crosstalk in 1.5- $\mu$ m InGaAsP optical amplifiers. *Journal of Lightwave Technology*, 6(10), 1559-1565. <https://doi.org/10.1109/50.7916>

---

### General rights

Copyright and moral rights for the publications made accessible in the public portal are retained by the authors and/or other copyright owners and it is a condition of accessing publications that users recognise and abide by the legal requirements associated with these rights.

- Users may download and print one copy of any publication from the public portal for the purpose of private study or research.
- You may not further distribute the material or use it for any profit-making activity or commercial gain
- You may freely distribute the URL identifying the publication in the public portal

If you believe that this document breaches copyright please contact us providing details, and we will remove access to the work immediately and investigate your claim.

# Crosstalk in 1.5- $\mu\text{m}$ InGaAsP Optical Amplifiers

H. E. LASSEN, MEMBER, IEEE, P. B. HANSEN, AND K. E. STUBKJAER, MEMBER, IEEE

**Abstract**—A dynamical model for multichannel amplification by near-traveling-wave optical amplifiers is presented, and results on crosstalk induced by either amplitude modulation or frequency modulation are given. The mechanisms influencing the crosstalk are especially the residual facet reflectivities and the detuning of the channels relative to the amplifier Fabry–Perot spectrum. Calculations of worst case crosstalk levels are included. The model is verified experimentally for amplitude modulated signals, and crosstalk levels up to  $-7$  dB are reported. For frequency modulated signals, estimated crosstalk is significantly lower and can be reduced by high quality facet coatings.

## I. INTRODUCTION

OPTICAL AMPLIFIERS may be useful as repeaters in coherent transmission systems with frequency division multiplexed channels because of their ability to amplify all channels simultaneously. For this application the crosstalk due to the amplifier is an important parameter. Previous work related to crosstalk in amplifiers includes reports on two-color gain saturation [1], [2] and interference from 1-kHz on-off switching of channels [3]. A two-channel experiment with direct detection systems was reported in [4] and a ten-channel PSK system with an optical amplifier [5] has also been demonstrated. Recently, results for four-wave mixing in amplifiers were reported [6] for very close channel spacing.

This paper presents a theoretical model for crosstalk between two simultaneously amplified channels, as well as an experimental verification of AM-induced crosstalk. The amplifiers investigated are near-traveling-wave amplifiers. As this type of amplifier does not put special restrictions on the transmitter wavelengths, it is considered the easiest to operate. In our experiments we used large channel separations ( $> 100$  GHz) and any beat phenomena between channels are therefore not considered.

Section II gives the details of the dynamical model, based on a slowly varying envelope approximation for the electric field waves within the optical amplifier and the injected light signals. We then give the definitions used in characterizing the crosstalk, and after outlining the numerical procedure, theoretical results on crosstalk induced by either amplitude or frequency modulation of one of the channels are presented. Next, the mechanisms influencing the crosstalk are identified, i.e., the input

powers, the residual facet reflectivities, and the signal frequencies relative to the frequencies of the residual Fabry–Perot modes of the amplifier. As the crosstalk is found to be especially sensitive to the latter, we also present the results of a worst case calculation, which can give some useful guidelines to the use of amplifiers. In Section III the experimental setup is presented and experimental results on amplitude modulation induced crosstalk for a near-traveling-wave optical amplifier are given. The measured crosstalk is found to be in qualitative agreement with the theoretical predictions.

## II. AMPLIFIER MODEL FOR TWO-CHANNEL AMPLIFICATION

In this section we first describe the dynamical amplifier model which is used for calculation of crosstalk and next the model is used to calculate both AM- and FM-crosstalk under different operating conditions. The AM-crosstalk can physically be interpreted as being mainly due to the gain modulation which is a result of the carrier depletion caused by the input signals. The FM-crosstalk can be understood by interpreting the residual Fabry–Perot modes of the amplifier as frequency discriminators. This FM/AM conversion causes the carrier density, and thereby the refractive index of the active region, to vary. The latter results in an unwanted phase-modulation of the signals.

### A. Dynamical Equations

The optical amplifier, which simultaneously amplifies two channels, is depicted in Fig 1. We consider two injected signals  $\hat{E}_1^i(t) = E_1^i(t) e^{i\omega_1 t}$  and  $\hat{E}_2^i(t) = E_2^i(t) e^{i\omega_2 t}$  with the carrier frequencies  $\omega_1$  and  $\omega_2$ , and slowly varying envelope functions  $E_1^i(t)$  and  $E_2^i(t)$ , respectively. In the following, the fields are treated independently for each of the channels. We thus neglect the influence of the beat between the two frequencies, and consider the signals to interact solely through the intensity-induced carrier depletion. Within the amplifier, the total field is composed of time- and space-dependent right and left traveling fields  $E_l^+(t, z)$  and  $E_l^-(t, z)$  for each of the signals. Throughout this paper, the subscript  $l$ , where  $l$  can take on the values 1 and 2, denotes the channel number. In the time domain, the boundary conditions for the fields take the form:

$$\begin{aligned} E_l^+(t, 0) &= E_l^i(t) + r_1 E_l^-(t, 0), & l = 1, 2 \\ E_l^-(t, L) &= r_2 E_l^+(t, L), & l = 1, 2 \end{aligned} \quad (1)$$

where  $r_1$  and  $r_2$  are the field reflectivities of the amplifier facets, and  $L$  is the length of the amplifier.

Manuscript received February 15, 1988; revised May 24, 1988.

H. E. Lassen was with the Electromagnetics Institute, Technical University of Denmark, DK-2800, Lyngby, Denmark. He is now with the Telecommunication Research Laboratory, DK-2970, Hørsholm, Denmark.

P. B. Hansen and K. E. Stubkjaer are with the Electromagnetics Institute, Technical University of Denmark, DK-2800, Lyngby, Denmark.

IEEE Log Number 8822718.

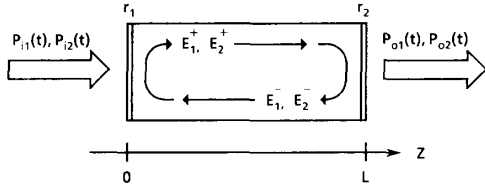


Fig. 1. Schematic diagram of optical amplifier simultaneously amplifying two channels.

By employing the usual slowly varying envelope approximation (expanding the complex wavenumber  $k(\omega, N)$  to first order around the carrier frequencies  $\omega_l$ ) and by assuming the carrier density  $N$  to vary slowly compared to the transit time for the fields in the cavity, (1) can be rewritten as

$$E_l^+(t, L) = r_1 r_2 e^{-i2k(\omega_l, N)L} E_l^+ \left( t - \frac{2n_g}{c} L \right) + e^{-ik(\omega_l, N)L} E_l^i \left( t - \frac{Ln_g}{c} \right), \quad l = 1, 2. \quad (2)$$

Here  $c$  is the velocity of light in vacuum,  $n_g$  is the effective group index for the waveguide, and  $k(\omega, N)$  is the complex wavenumber given by:

$$k(\omega, N) = \frac{\omega}{c} n(\omega, N) + i \frac{1}{2} (g(N) - \alpha_i) \quad (3)$$

where  $n(\omega, N)$  is the effective refractive index for the active layer, and  $g(N)$  and  $\alpha_i$  are the modal power gain and internal loss per unit length. Introducing the short-hands

$$E_l^o(t) \equiv E_l^+(t, L) \quad (4)$$

and

$$e^{-ik(\omega_l, N)L} = g_c e^{-i\delta_l}, \quad l = 1, 2 \quad (5)$$

and denoting the transit-time  $Ln_g/c$  by  $\tau$ , (2) takes the form of a recursion formula for an active Fabry-Perot resonator:

$$E_l^o(t) = r_1 r_2 g_c^2 e^{-i2\delta_l} E_l^o(t - 2\tau) + g_c e^{-i\delta_l} E_l^i(t - \tau), \quad l = 1, 2. \quad (6)$$

Here  $g_c$  is a complex single-pass field gain, and the phase-shifts  $\delta_l$  account for the differences between the (optical) signal-frequencies  $\omega_l$  and the frequency  $\omega_r$  of a reference cavity resonance

$$\delta_l = (\omega_l - \omega_r) \tau, \quad l = 1, 2. \quad (7)$$

The frequency  $\omega_r$  is a resonance frequency of the amplifier at the reference carrier density  $N_r$ , which, in this case, is chosen to be the carrier density at lasing threshold for an uncoated laser. In the following, the term "detuning" will be used for  $\delta_l$ . In the case of static operation (6) reduces to the well known Fabry-Perot formula.

The complex single-pass field gain is defined as

$$g_c = \sqrt{G_s} e^{i\Phi} \quad (8)$$

where  $G_s$  is a single-pass power gain given by

$$G_s = e^{(g(N) - \alpha_i)L} = e^{(\Gamma A(N - N_o) - \alpha_i)L}. \quad (9)$$

Here  $\Gamma$  is the confinement factor for the intensity of the fundamental waveguide mode,  $A$  is the active layer gain coefficient, and  $N_o$  is the transparency carrier concentration. The gain model is only dependent on the carrier density, i.e., nonlinear gain phenomena [7] are not included. The single-pass phase shift  $\Phi$  appearing in the expression for the complex field gain, (8) is due to the change of the effective refractive index  $n(\omega, N)$  with the carrier density

$$\Phi = \frac{\omega}{c} L \frac{\partial n(\omega, N)}{\partial N} (N - N_r) = \frac{1}{2} \Gamma A (N - N_r) L \alpha. \quad (10)$$

Here  $\alpha$  describes the variation of refractive index with carrier density relative to the variation of the gain:

$$\alpha = -\frac{2\omega}{c} \left( \frac{\partial n(\omega, N)}{\partial N} \right) / \left( \frac{\partial g(N)}{\partial N} \right). \quad (11)$$

The parameter  $\alpha$  is also known as the linewidth enhancement factor [8].

The input powers  $P_l^i(t)$  and output powers  $P_l^o(t)$  indicated in Fig. 1 are related to the amplitudes of the envelopes of the input fields  $|E_l^i(t)|$  and output fields  $|E_l^o(t)|$  through

$$|E_l^i(t)|^2 = \zeta \frac{2(1 - r_1^2)}{wd/\Gamma} P_l^i(t), \quad l = 1, 2 \quad (12)$$

and

$$|E_l^o(t)|^2 = \zeta \frac{2}{(1 - r_2^2)wd/\Gamma} P_l^o(t), \quad l = 1, 2. \quad (13)$$

In (12) and (13),  $\zeta = \sqrt{\mu_o/\epsilon_o}/n(\omega, N)$  is the wave impedance, where  $\epsilon_o$  is the vacuum permittivity and  $\mu_o$  is the vacuum permeability. The effective area of the guided mode is given by  $wd/\Gamma$ , where  $w$  and  $d$  are the waveguide width and thickness, respectively. By inclusion of the transmission coefficients  $(1 - r_1^2)$  and  $(1 - r_2^2)$ , the reference planes for the field amplitudes in (12) and (13) have been chosen to be immediately inside the facets of the amplifier. Coupling losses are not accounted for.

To evaluate the carrier density  $N$ , the usual rate equation is employed:

$$\frac{dN}{dt} = \frac{I_{th}}{ewdL} \frac{I}{I_{th}} - R(N) - A(N - N_o) \frac{c}{n_g} S. \quad (14)$$

Here  $I_{th}$  is the injection current at lasing threshold of the uncoated amplifier and  $I/I_{th}$  is the normalized injection current.

For the recombination rate  $R(N)$  we use a detailed model [9]:

$$R(N) = aN + bN^2 + cN^3 \quad (15)$$

where  $a$ ,  $b$ , and  $c$  are constants. Previous work [10], [11] on optical amplifiers based on InGaAsP semiconductor lasers, has made clear the significant influence of the non-radiative Auger recombination on the performance of the optical amplifiers at relatively high current densities.

The total average photon density  $S$  is the sum of the contributions from the amplified signals  $S_{\text{sig}}$  and amplified spontaneous emission  $S_{\text{sp}}$ :

$$S = S_{\text{sig}} + S_{\text{sp}} \quad (16)$$

Assuming the variation in carrier density over a time period of a transit time  $\tau$  to be negligible, the averaging procedure described in [12] can be used to find the average photon densities:

$$S_{\text{sig}} = \frac{G_s - 1}{G_s \ln G_s} \frac{1 + r_2^2 G_s n_g}{1 - r_2^2} \sum_{l=1,2} \frac{1}{c} \frac{P_l^o}{\hbar \omega_l w d / T} \quad (17)$$

$$S_{\text{sp}} = \frac{\beta R(N) \tau}{2 \ln G_s} \left( \frac{((r_1^2 + r_2^2) (G_s - 1) + 2(1 - r_1^2 r_2^2 G_s)) (G_s - 1)}{(1 - r_1^2 r_2^2 G_s^2) \ln G_s} - 2 \right) \quad (18)$$

Here  $\hbar$  is the reduced Planck's constant and  $\beta$  is the fraction of spontaneous emission coupled into the guided modes.

The recursion formula (6), can describe ultrahigh speed dynamical properties of optical amplifiers. Time-varying phenomena with durations down to the order of one transit time  $\tau$  ( $\approx 6$  ps), e.g., amplification of picosecond pulses, are expected to be the intrinsic limit for the validity of the model. Here we use the model to study the effect of either amplitude- or frequency modulation of the input signals with modulation frequencies of the order of a few hundred megahertz.

### B. Crosstalk Definitions

In the case of amplitude modulation, the input power of channel 1 is modulated at a frequency  $\Omega$  while the input power of channel 2 is kept constant. At the output, the signals from the two channels take the form

$$P_l^o(t) = P_{l0}^o + \sum_{m=1}^{\infty} P_{lm}^o \cdot \sin(m\Omega t + \Phi_{lm}), \quad l = 1, 2 \quad (19)$$

where  $P_{l0}^o$  is the constant output power level, and  $P_{lm}^o$  and  $\Phi_{lm}$  are the amplitude and phase of the  $m$ th harmonic. The general expression (19) includes crosstalk in channel 2 as well as harmonic distortion in channel 1. As a measure for the AM-crosstalk  $\gamma_{\text{AM}}$  we use the ratio of the spurious modulation appearing in channel 2 to the intentionally imposed modulation in channel 1:

$$\gamma_{\text{AM}} = \frac{P_{21}^o}{P_{11}^o} \quad (20)$$

In the case of frequency modulation, the input powers are constant for both channels, while the phase-angle of the complex envelope of the input field for channel 1 is sinusoidally modulated at a frequency  $\Omega$ . At the output, the phase angles  $\Psi_l^o(t)$  take the form:

$$\Psi_l^o(t) = \Psi_{l0}^o + \sum_{m=1}^{\infty} \beta_{lm}^o \sin(m\Omega t + \Psi_{lm}^o), \quad l = 1, 2 \quad (21)$$

where  $\Psi_{l0}^o$  is a constant phase shift and  $\beta_{lm}^o$  and  $\Psi_{lm}^o$  are the FM-indices and phases of the  $m$ th harmonic of the phase modulation.

Similar to the above case of amplitude modulation, we will in this case define the FM-crosstalk  $\gamma_{\text{FM}}$  as:

$$\gamma_{\text{FM}} = \frac{\beta_{21}^o}{\beta_{11}^o} \quad (22)$$

### C. Numerical Results

The crosstalk is calculated by the numerical solution of (6)–(18) in the time domain followed by Fourier analysis of the results. The amplifier is characterized by the parameters given in Table I. Fig. 2(a) shows the AM-crosstalk  $\gamma_{\text{AM}}$  versus the detuning for two different pumping levels  $I/I_{\text{th}} = 3.2$  and  $I/I_{\text{th}} = 3.4$ . The modulation frequency is 500 MHz, the average input power for each of the channels is  $-30$  dBm, and the AM-index  $m_{\text{AM}} = P_{11}^i/P_{10}^i$  is 0.5. In this example we used equal detuning for the two channels ( $\delta_1 = \delta_2$ ) but calculations with different detunings ( $\delta_1 \neq \delta_2$ ) exhibit a similar behavior with dips in the crosstalk versus detuning. According to a small-signal analysis [13], the dips in the crosstalk will only occur for single-pass gain levels  $G_s$  fulfilling:

$$G_s > \frac{1}{2\alpha r_1 r_2} \quad (23)$$

With the chosen parameters, the single-pass gain should be higher than 16.5 dB. The dips occur at the values of the detuning, where the carrier-induced gain modulation is compensated by the carrier-induced shift of the residual Fabry-Perot modes. The carrier-variation in turn is caused by the time varying intensity in channel 1. In the limit of vanishing facet reflectivities, the residual mode structure and therefore also the dips will disappear and in addition the crosstalk will be approximately proportional to the gain.

Similarly, the FM crosstalk versus detuning is shown in Fig. 2(b). The conditions are the same as above in Fig. 2(a), except that channel 1 is frequency modulated at 500 MHz with a FM-index  $\beta_1^i = 1.0$ . The FM crosstalk is

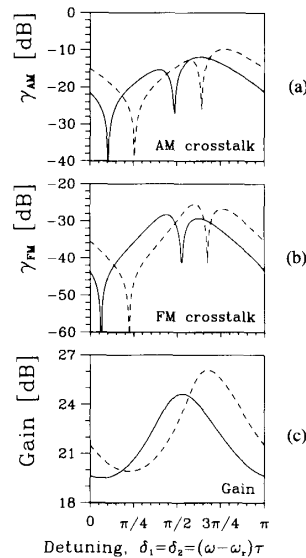


Fig. 2. Calculated crosstalk and gain versus detuning for two pumping levels:  $I/I_{th} = 3.2$  (—) and  $I/I_{th} = 3.4$  (---). (a) AM crosstalk for  $m_{AM} = 0.5$ . (b) FM crosstalk for  $\beta_1^2 = 1.0$ . (c) Gain for each channel. In all cases:  $\delta_1 = \delta_2$ ,  $P_{10} = P_{20} = -30$  dBm, and modulation frequency 500 MHz.

TABLE I  
LIST OF PARAMETER VALUES

Symbol	Parameter	Value
a	recombination coefficient	$1 \cdot 10^{16} \text{ m}^{-3} \text{ s}^{-1}$
b	recombination coefficient	$1 \cdot 10^{16} \text{ m}^{-3} \text{ s}^{-1}$
c	recombination coefficient	$5 \cdot 10^{11} \text{ m}^{-3} \text{ s}^{-1}$
$\beta$	spontaneous emission factor	$2 \cdot 10^{-4}$
$\alpha$	linewidth enhancement factor	5.6
L	amplifier length	500 $\mu\text{m}$
d	active layer thickness	0.2 $\mu\text{m}$
w	active region width	2 $\mu\text{m}$
$\Gamma$	confinement factor	0.3
$\alpha_i$	internal loss	2000 $\text{m}^{-1}$
n	refractive index	3.5
$n_g$	group index	3.75
A	gain factor	$2.6 \cdot 10^{20} \text{ m}^2$
$N_0$	carrier density at transparency	$1.09 \cdot 10^{24} \text{ m}^{-3}$
$N_r$	reference carrier density	$1.61 \cdot 10^{24} \text{ m}^{-3}$
$I_{th}$	threshold current for uncoated amplifier	16.5 mA
$r_1^2$	residual facet reflectivity	$2 \cdot 10^{-3}$
$r_2^2$	residual facet reflectivity	$2 \cdot 10^{-3}$

simpler in nature and is dominantly due to the changing refractive index with carrier density. The carrier variation is a result of the FM/AM conversion originating from the frequency discriminator effect of the residual Fabry-Perot modes of the amplifier. This FM/AM conversion vanishes at the extremes of the Fabry-Perot modes, as seen from the dips in the curves of Fig. 2(b), and eventually disappears for vanishing facet reflectivities. Fig. 2(c) shows the gain of the amplifier versus detuning for the cases shown in Fig. 2(a) and (b). As the detunings are equal for

the two channels ( $\delta_1 = \delta_2$ ), the gain is identical for the two channels and to a very good approximation also independent of the modulation scheme. The asymmetry of the Fabry-Perot modes due to the changes in refractive index with carrier density is clearly seen.

As both the AM crosstalk and FM crosstalk are found to be very sensitive to the detuning of the two channels and to the residual facet reflectivities, we have carried out worst case calculations. By worst case we understand the maximum crosstalk which results when the detunings  $\delta_1$  and  $\delta_2$  are varied independently over intervals of  $\pi$ . Fig. 3 gives the maximum obtainable AM and FM crosstalk versus gain for input powers of  $-30$  dBm to each channel and for facet reflectivities of  $r_1^2 = r_2^2 = 2 \times 10^{-3}$  (solid curves),  $10^{-3}$  (dotted curves), and  $10^{-4}$  (dashed curves). The results are obtained at bias levels for which the unsaturated gain ripple is smaller than 5 dB. For the high facet reflectivity of  $2 \times 10^{-3}$  the AM crosstalk is proportional to the gain while the FM crosstalk is proportional to the square of the gain until the gain reaches a level determined by (23). Beyond this level the crosstalk increases more rapidly with gain until a saturation level marked by the vertical lines is reached. For gain levels exceeding this limit, the amplifier can only be operated with restrictions as far as the detuning (frequency) of the input signals is concerned (when also fulfilling the requirement of a maximum gain ripple of 5 dB). In both the AM and FM case, the crosstalk can be reduced by reducing the facet reflectivities, but only in the case of frequency modulation can the crosstalk be reduced to insignificant levels. A reflectivity of  $2 \times 10^{-3}$  is readily obtained with presently available AR-coating techniques whereas a reflectivity of  $10^{-4}$  is among the best reflectivities reported for amplifier AR coats.

Fig. 4 gives the maximum obtainable AM and FM crosstalk versus input power to each channel ( $P_{10} = P_{20}$ ) for a fixed gain of 20 dB and for facet reflectivities of  $r_1^2 = r_2^2 = 2 \times 10^{-3}$  (solid curves) and  $10^{-4}$  (dashed curves). In both the AM and FM case, the crosstalk is proportional to the input power. System penalties of 1 and 0.1 dB result for crosstalk levels of  $-10$  and  $-17$  dB, respectively [14]. A penalty of 0.1 dB is considered acceptable for systems applications and from Fig. 4 it is seen that for 20-dB gain the input power should be lower than  $-33$  dBm ( $r_1^2 = r_2^2 = 2 \times 10^{-3}$ ) and  $-24$  dBm per channel ( $r_1^2 = r_2^2 = 10^{-4}$ ) in order to avoid serious penalty due to AM crosstalk. On the contrary the FM crosstalk will not imply any restrictions for realistic input power levels at a 20-dB gain.

For comparison, Westlake and O'Mahony reported [4] the power penalty due to crosstalk in a direct detection system to be negligible for input powers of  $-22.5$  dBm in the case of a 19-dB gain in an amplifier with facet reflectivities of  $10^{-3}$ . According to Fig. 3 (taking the crosstalk to be linear with input power) we predict an AM crosstalk of  $-13$  dB and therefore a penalty of 0.4 dB for the same gain, input power, and facet reflectivities. Considering the uncertainties in parameters, our results are

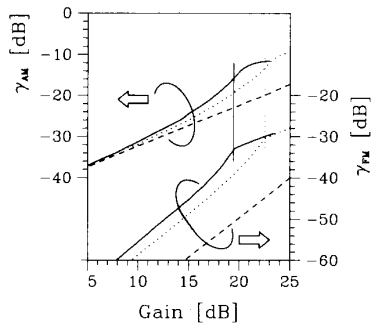


Fig. 3. Worst case AM and FM crosstalk versus gain in channel 2 for  $P_{10}^i = P_{20}^i = -30$  dBm and modulation frequency of 500 MHz. The facet reflectivities are  $2 \times 10^{-3}$  (—),  $10^{-3}$  (····), and  $10^{-4}$  (----). (AM case:  $m_{AM} = 0.5$ , FM case:  $\beta_1^i = 1.0$ .)

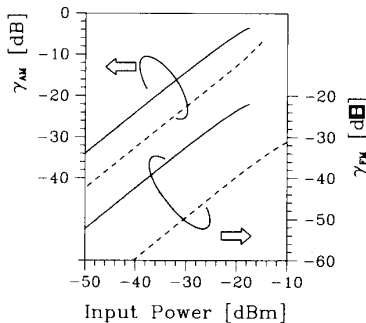


Fig. 4. Worst case AM and FM crosstalk versus input power to each channel ( $P_{10}^i = P_{20}^i$ ) for 20-dB gain (channel 2) and modulation frequency of 500 MHz. The facet reflectivities are  $2 \times 10^{-3}$  (—) and  $10^{-4}$  (----). (AM-case:  $m_{AM} = 0.5$ , FM-case:  $\beta_1^i = 1.0$ .)

considered to be in acceptable agreement with these experimental results.

The crosstalk is dependent on the modulation frequency and according to a small-signal analysis [13] the AM crosstalk has a low-pass characteristic and the FM crosstalk a high-pass characteristic. Both have the same 3-dB frequency which is largely determined by  $dR(N)/dN$ , which can be interpreted as the dynamic carrier lifetime. For an amplifier gain of 20 dB the 3-dB frequency will be approximately 375 MHz.

### III. MEASUREMENTS

#### A. Experimental Setup

Measurements of AM crosstalk are performed using the setup shown schematically in Fig. 5. As sources for the two-channel experiments we use single-mode external cavity lasers as depicted in Fig. 6. The external cavity lasers are based on 1.52- $\mu\text{m}$  DCPBH lasers AR-coated on one facet. Since we only have access to one facet the light is coupled from the cavity lasers into a single-mode fiber using the zero-order Bragg reflection of the grating and a microscope objective. The threshold current for the solitary laser was 16.5 mA before AR-coating and 30 mA after AR-coating. A tuning range of approximately 100 nm has been obtained, as can be seen from the measured threshold current versus wavelength shown in Fig. 7. The

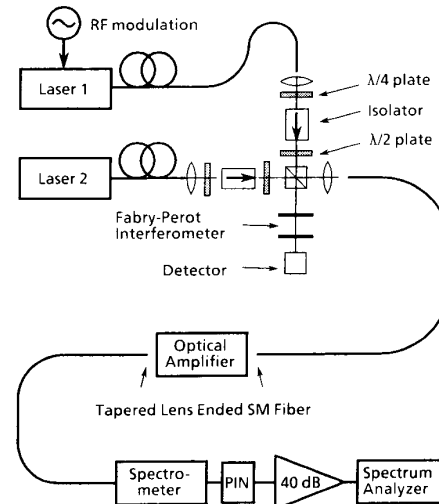


Fig. 5. Experimental setup.

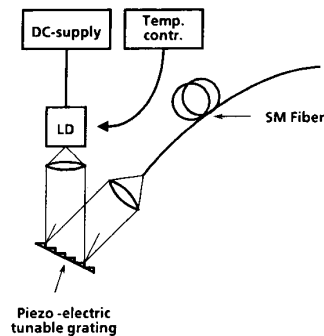


Fig. 6. External cavity laser arrangement.

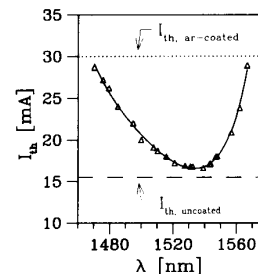


Fig. 7. Threshold current versus wavelength for external cavity laser depicted in Fig. 6. Threshold of solitary uncoated laser is indicated by (----). Threshold of solitary AR-coated laser is indicated by (····).

optical amplifiers are 500- $\mu\text{m}$ -long 1.52- $\mu\text{m}$  DCPBH lasers and AR coated on both facets. The AR coatings are produced using single-layer *e*-beam evaporation of zirconium oxide and titanium oxide, which reproducibly results in residual power facet reflectivities of the order of  $2 \times 10^{-3}$ .

One of the sources is RF modulated. Optical isolators are used to reduce the interaction between the laser sources and the amplifier, especially being a problem when the latter at high gain levels is operated close to its lasing threshold. Using quarter-wave and half-wave retarder plates before and after the isolators, respectively, and

tatable mounts for the latter, the transmission loss for the isolator is minimized and gives us the ability to control the direction of polarization for the linearly polarized light from the isolators. The two signals are coupled into one single-mode fiber using a beamsplitter, and from the other branch of the beamsplitter, the light is coupled through a scanning Fabry-Perot interferometer, which is used for monitoring the external cavity lasers. The light is coupled into and out from the optical amplifier using tapered lens endings, with coupling efficiencies of typically 25–30 percent. On the output side of the optical amplifier, the single-mode fiber is coupled to a grating spectrometer for spectral filtering of the two channels. Their wavelength separation is of the order of one amplifier-cavity mode spacing. After having filtered out one of the channels, the RF content of the optical power is in turn measured using a Ge p-i-n diode, 40 dB of amplification, and a HP8566 RF spectrum analyzer.

### B. AM Crosstalk Measurements

For two different modulation frequencies and channel spacings, we show in Figs. 8 and 9 measured and calculated AM crosstalk and gain versus normalized injection current  $I/I_{th}$ . The input wavelengths are approximately  $1.474 \mu\text{m}$  which matches the gain maximum at high injection levels. The channel separations are 14.5 and  $9.6 \text{ \AA}$  (corresponding to 2.4 and 1.6 times the amplifier cavity mode spacing) and the modulation frequencies are 100 and 500 MHz for the two experiments shown in Figs. 8 and 9, respectively. In both cases, the powers coupled into the amplifier are estimated to be  $-24$  and  $-30$  dBm for the modulated and unmodulated channels, respectively. Measurements of AM crosstalk are indicated with markers in Figs. 8(a) and 9(a), while calculations of AM crosstalk are shown as full curves. The corresponding measured gain levels for the modulated channel are indicated with markers in Figs. 8(b) and 9(b), while calculated gain levels for the modulated and unmodulated channel are shown as full and dashed curves, respectively. The channel separations are measured using the spectrometer and are also given in terms of amplifier cavity mode spacings, as that directly gives the differences in detunings, i.e.,  $|\delta_1 - \delta_2| = 0.4\pi$  and  $|\delta_1 - \delta_2| = 0.6\pi$  for the two cases. The two experiments clearly illustrate the critical dependency of the crosstalk on the detunings relative to the residual amplifier modes, which are moving towards shorter wavelengths with increasing injection current. In the case of  $|\delta_1 - \delta_2| = 0.4\pi$ , the crosstalk decreases with increasing injection current at high current levels, while it increases in the case, where  $|\delta_1 - \delta_2| = 0.6\pi$ . The qualitative agreement between measurements and calculations was obtained by keeping the differences between the detunings constant, as indicated above, and sweeping the frequencies of the two channels relatively to the gain spectrum of the amplifier. Considering the uncertainties on estimating experimental conditions as well as amplifier parameters, we find the agreement between measurements and theory to be acceptable.

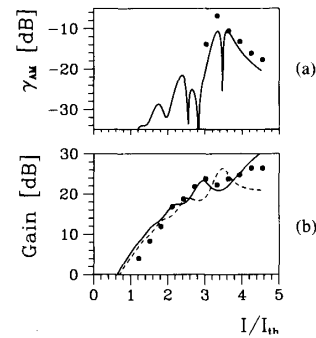


Fig. 8. Measured and calculated AM crosstalk and gain versus injection current. (a) Measured ( $\bullet$ ) and calculated (—) crosstalk. (b) Measured ( $\bullet$ ) and calculated (—) gain for channel 1. Calculated gain for channel 2 indicated by (---).  $P_{10} = -24$  dBm and  $P_{20} = -30$  dBm. Channel separation  $14.5 \text{ \AA}$ . Modulation frequency 100 MHz.

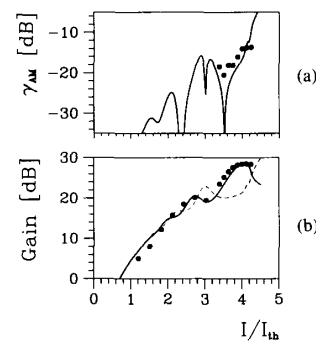


Fig. 9. (a) (b) As Fig. 8, but with channel separation  $9.6 \text{ \AA}$  and modulation frequency 500 MHz.

### IV. CONCLUSION

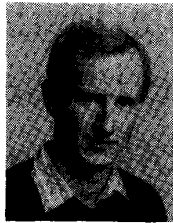
A dynamical model for a near-traveling-wave optical amplifier was established. The model is based on field equations for the injected light and intracavity light and it enables calculation of AM and FM crosstalk between simultaneously amplified channels. Residual facet reflectivities and channel frequencies relative to the Fabry-Perot resonances of the amplifier were identified as factors which have a strong influence on the crosstalk. The worst case crosstalk was calculated versus gain and input power. In the case of amplitude modulation, crosstalk levels of up to  $-14$  dB were found for a gain of 20 dB with input powers of  $-30$  dBm per channel and realistic facet reflectivities of  $2 \times 10^{-3}$ . These crosstalk levels can be prohibitive for multichannel amplification of AM signals and cannot be largely reduced by improved AR coatings. The FM crosstalk levels on the other hand were found to be acceptable, i.e.,  $-32$  dB for 20 dB gain, and can be reduced further to insignificant levels by use of high quality AR coatings ( $R \approx 10^{-4}$ ). Experimentally, we have characterized the AM crosstalk which was measured to be as high as  $-7$  dB. Generally, we found acceptable agreement between theoretically and experimentally determined AM crosstalk versus injection current to the amplifier.

## ACKNOWLEDGMENT

The authors would like to thank the Opto-Electronics Group and Dr. P. A. Kirkby, Dr. G. D. Henshall, and Dr. A. J. Collar of STC Technology, Harlow, England, for kindly supplying the laser diodes. H. Olesen and B. Tromborg of the Telecommunication Research Laboratory are acknowledged for stimulating discussions, and the authors are indebted to their colleagues B. F. Jørgensen, for preparing the tapered fibers, and B. Mikkelsen, for supplying data on the external cavity lasers.

## REFERENCES

- [1] G. Eisenstein *et al.*, "Two-color gain saturation in an InGaAsP near-traveling-wave optical amplifier," in *Tech. Dig. OFC/IOOC 1987* (Reno, Nevada), 1987, vol. 3, p. 199.
- [2] T. Mukai, K. Inoue, and T. Saitoh, "Signal gain saturation in two-channel common amplification using a 1.5- $\mu\text{m}$  InGaAsP traveling-wave laser amplifier," *Electron. Lett.*, vol. 23, pp. 396-397, 1987.
- [3] G. Grosskopf, R. Ludwig, and H. G. Weber, "Crosstalk in optical amplifiers for two-channel transmission," *Electron. Lett.*, vol. 22, pp. 900-901, 1986.
- [4] H. J. Westlake and M. J. O'Mahony, "Bidirectional and two-channel transmission system measurements using a semiconductor-laser-amplifier repeater," *Electron. Lett.*, vol. 23, pp. 649-650, 1987.
- [5] R.-P. Braun, R. Ludwig, and R. Molt, "Ten-channel coherent optic fiber transmission using an optical traveling wave amplifier," in *Tech. Dig. ECOC'86* (Barcelona, Spain), vol. 3, pp. 29-32.
- [6] K. Inoue, T. Mukai, and T. Saitoh, "Nearly degenerate four-wave mixing in a traveling-wave semiconductor laser amplifier," *Appl. Phys. Lett.*, vol. 51, pp. 1051-1052, 1987.
- [7] J. E. Bowers, T. L. Koch, B. R. Hemenway, D. P. Wilt, T. L. Bridges, and E. G. Burkhardt, "High-frequency modulation of 1.52  $\mu\text{m}$  vapor-phase-transported InGaAsP lasers," *Electron. Lett.*, vol. 21, pp. 297-299, Mar. 1985.
- [8] C. H. Henry, "Theory of the linewidth of semiconductor lasers," *IEEE J. Quantum Electron.*, vol. QE-18, pp. 259-264, Feb. 1982.
- [9] R. Olshansky, C. B. Su, J. Manning, and W. Powazinik, "Measurement of radiative and nonradiative recombination rates in InGaAsP and AlGaAs light sources," *IEEE J. Quantum Electron.*, vol. QE-20, pp. 838-854, Aug. 1984.
- [10] M. J. O'Mahony, "Semiconductor laser amplifiers as repeaters," in *Tech. Dig. IOOC-ECOC'85* (Venezia, Italy), Oct. 1-4, 1985, vol. II, pp. 39-46.
- [11] J. W. Wang, H. Olesen, and K. E. Stubkjaer, "Recombination, gain, and bandwidth characteristics of 1.3- $\mu\text{m}$  semiconductor laser amplifiers," in *Tech. Dig. IOOC-ECOC'85* (Venezia, Italy), Oct. 1-4, 1985, vol. I, pp. 157-160.
- [12] M. J. Adams, J. V. Collins, and I. D. Henning, "Analysis of semiconductor laser optical amplifiers," *Proc. Inst. Elec. Eng.*, vol. 132, pt. J, pp. 58-63, Feb. 1985.
- [13] H. E. Lassen, work to be published.
- [14] G. P. Agrawal, "Evaluation of crosstalk penalty in multichannel ASK heterodyne optical communication systems," *Electron. Lett.*, vol. 23, pp. 906-908, 1987.

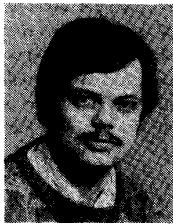


devices.

**Hans Erik Lassen** (S'84, M'87) was born in Sønderborg, Denmark, in 1958. He received the M.Sc. degree from the Electromagnetics Institute, Technical University of Denmark, in 1984. From 1984 to 1986 he was with the Electromagnetics Institute on a Ph.D. scholarship.

From 1986 to 1988 he was an Assistant Professor with the Electromagnetics Institute. He is now with the Telecommunication Research Laboratory, Hørsholm, Denmark, working on nonlinear dynamics of semiconductor lasers and related

\*



tories, Crawford Hill, NJ.

**Per Bang Hansen** was born in Assens, Denmark, on March 17, 1961. In 1986 he received the M.Sc. degree in electrical engineering from the Technical University of Denmark, where he is currently working towards the Ph.D. degree. The main theme of his studies is optical semiconductor amplifiers.

In 1985 and 1986 he worked at NEC Central Research Laboratories, Kawasaki, Japan, as a Guest Researcher. Since February 1988 he has been a Visiting Scientist at AT&T Bell Laboratories, Crawford Hill, NJ.

\*



**Kristian E. Stubkjaer** (S'76-M'81) was born in Århus, Denmark, in 1953. He received the M.Sc. and Ph.D. degrees from the Technical University of Denmark, Copenhagen, in 1977 and 1981, respectively.

From 1979 to 1981 he studied at the Tokyo Institute of Technology, Tokyo, Japan, with a scholarship from the Japanese Government. From 1981 to 1982 he was drafted for military service at the Danish Defence Research Establishment in Copenhagen. From 1982 to 1983 he was a Visiting Scientist at the IBM T. J. Watson Research Center, Yorktown Heights, NY. He is now an Associate Professor at the Electromagnetics Institute, Technical University of Denmark, Lyngby, Denmark, where he is working in the field of optical communication. Since June 1985 he has been Director of the Electromagnetics Institute.